

A STUDY OF THE METHOD FOR MEASURING THE LOCAL SIZE DISTRIBUTION OF SPHERICAL PARTICLES DIFFUSING IN A FLUID BY L.D.A.

Suck Ju Yoon*

(Received June 27, 1987)

This work concerns a method for measuring the local size distribution of spherical particles diffusing in a fluid. It is based on the light scattering theory and makes use of an ordinary Laser Doppler Anemometry apparatus. The required information is obtained by analyzing and processing the signal from the PM, which observes the measuring volume at the angle of 90° . The pinhole is replaced by a slit oriented in such a way that the intensity of the scattered light depends only on the diameter of the particle and on a single space variable. A direct calibration of the response of the optical system is used to compute the size distribution from the scattered light probability density.

Key Words : Particle Size Distribution, Particle Diffusion, Optical Measurement, Laser Doppler Velocimeter

1. INTRODUCTION

Much research has been going on over the past years to find ways of measuring the statistical size distribution of a set of particles. It can be highly advantageous to extract this information from the light scattered by the particles as they pass through the probe volume of a Doppler effect laser anemometer, as we can then hope to find not only the size distribution but also the velocity of the particles. Generally, the methods proposed can be broken down roughly into two categories: those that deduce the size of the particles, assumed to be spherical, from the fringe visibility (Farmer, W.M., 1972) and those based on the diffusion theory of spherical particles (Mie, G., 1908; Van de Hulst, H. C., 1957), which find the particle diameter from the pedestal value of the *PM* output signal (Umhauer, H., 1975; Yule, A.J., et al. 1977).

The method described here belongs to the latter category. It has the advantage of using conventional laser velocimetry to extract the desired information from the *PM* output signal. It is based on two elements: a special arrangement of the optical system that simplifies the interpretation of the optical signal and a calibration of system response, which can be done in situ, to deconvolute the directly observed statistical distribution by processing the electrical signal from the photosensor.

2. PRINCIPLE

In a monochromatic laser velocimetry setup, the initial laser beam is divided into two beams of roughly the same intensity. These are sent through a device that bends the beams, making them cross each other. Interference fringes

form in the volume of the intersection, or probe volume, which consists of ideally parallel planes. The extent of the probe volume depends on the diameter of the beams and on the angle between them.

The distance separating the fringes is a function of the light wavelength and of the angle between the beams. Given the geometrical configuration of the optical system and the nature of laser light, we can calculate this interfringe space, estimate the extent of the probe volume and, thus, the number of fringes it contains. These elements can be modified independently by inserting certain simple devices in the optical path.

The probe volume is simplified to an ellipsoid shape (Fig. 1) with the meridian *y-z* plane coinciding with the plane common to the incident beams. The point of intersection of the two beam axes is the point of origin 0. The fringes are slices parallel to the *x-y* equatorial plane. The fringe intensity decreases uniformly starting at the equatorial plane, so that by simplifying we can represent the local light intensity

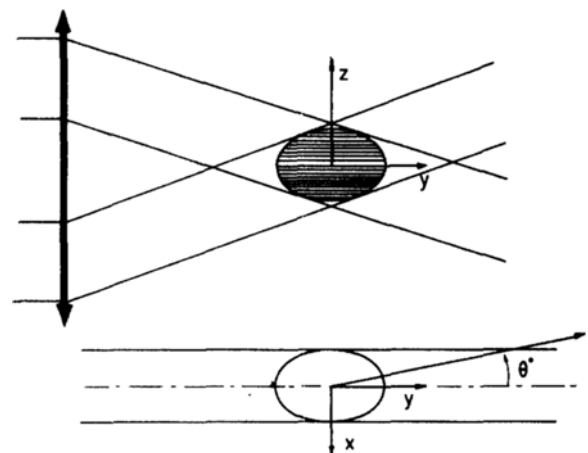


Fig. 1 Probe volume geometry

*Department of Mechanical Engineering, Chonbuk National University, Chonju 520, Korea

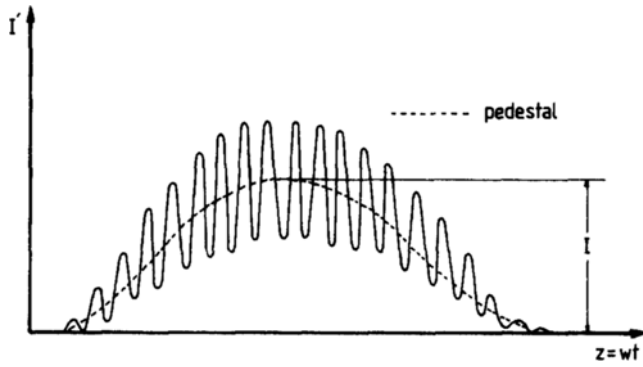


Fig. 2 Photomultiplier signal

I'' as we move along the x axis by a rake enveloped with a symmetrical distribution. Thus when a spherical particle of diameter D passes through the probe volume it diffuses light in a given direction and an intensity I' which, as a function of z , looks like the curve in Fig. 2. We choose here the special case where the diameter D is larger than the interfringe space i , which explains why I' does not attain zero values when the center of the particle is in the median plane of a black fringe. when the particle is in uniform rectilinear motion in the probe volume, the PM signal is recorded as a function of time, and if w is the z component of the particle velocity, the space-time function is $z = wt$.

The signal in Fig. 2 can be considered as two superimposed component: the high-frequency signal f_D , or Doppler signal, giving the value for w from the interfringe distance, and a lower-frequency pedestal signal, the amplitude of which depends on the position where the particle passed through the equatorial plane. when there are enough fringes in the probe volume, the pedestal and Doppler signal frequency bands are very far apart, and the Doppler signal can be filtered out without altering the pedestal signal. We will assume here that this has already been done. The analysis then concerns only the pedestal signal, which thus simulates a continuous equivalent distribution of light in the probe volume.

It is known that when a transparent sphere is illuminated by monochromatic light of wavelength λ and intensity I'' , the intensity, I' of the light which diffuses depends on the angle θ , measured from the direction of the incident light under which it is observed, on I'' and on the diameter of the sphere D .

The refractive indices of the sphere and the medium around the sphere also play a role, but will here be considered constant, taken into account implicitly in the relation

$$I' = f(I'', \theta, D) \tag{1}$$

θ can be eliminated by observing from the same angle at all times. Experiments then show that, under certain conditions, I' can be expressed by

$$I' = cI'' \left(\frac{D}{D_0} \right)^\alpha \tag{2}$$

Where c is a constant expressing the effects of θ , of the refractive indices and of other parameters. D_0 is a reference diameter and α is a positive real number. As distribution of the light is not uniform inside the probe volume, I''

depends on the position of the sphere within the volume, whence

$$I' = cI''(x, y, z) \left(\frac{D}{D_0} \right)^\alpha \tag{3}$$

The pedestal signal thus represents this function for a particle of diameter D moving parallel to the x axis. I' reaches a maximum at the passage through the equatorial plane, and the effect of z is eliminated when only this maximum value, denoted I , is of interest, as is the case here. The previous relation reduces to an expression in the form

$$I = c'I''(x, y) \left(\frac{D}{D_0} \right)^\alpha \tag{4}$$

Which shows that it is not possible to deduce the diameter D of the sphere from the measurement of I when the coordinated (X, Y) of the point where it passes through the equatorial plane are known.

The nature of the Eq.(4) can determined by a calibration. The optical axis of the PM is in the x - y plane at an angle θ from the y axis as shown in Fig. 1. The plane of the incident laser beam axis is perpendicular to the x - y plane. The same PM was used for two angles ($\theta=10^\circ$ and $\theta=90^\circ$)

A sample of spherical glass microballs with diameters going from 70 to 280 μm are glued to a point on glass sheets, and the assembly is mounted on a disk.

The disk axis is located approximately in the x - y plane, parallel to the y axis, and rotates in a bearing that can be translated parallel to the x and y axis. The circular path of the balls thus cuts orthogonally through the equatorial plane of the probe volume and the bearing can be moved to set the point of intersection at known coordinates. The value of the light I diffused by particles of different size as they pass through the equatorial plane is measured, as a function of x when $y=0$, then as a function of y for $x=0$. As an example, Fig. 3 shows the data obtained from three glass spheres of different diameters for an angle θ of 10° . The value for I is expressed in relation to the intensity I_c scattered by the particle when it passes point 0. σ_x and σ_y are the standard deviations of the values for x and y , respectively. If we allow that the surfaces of equal light intensity I' are

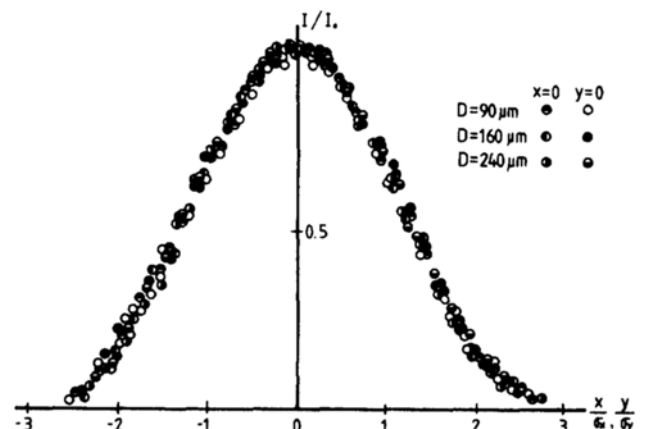


Fig. 3 Variation in the scattered light as a function of the point at which the particle passes through the equatorial plane, for $\theta=10^\circ$

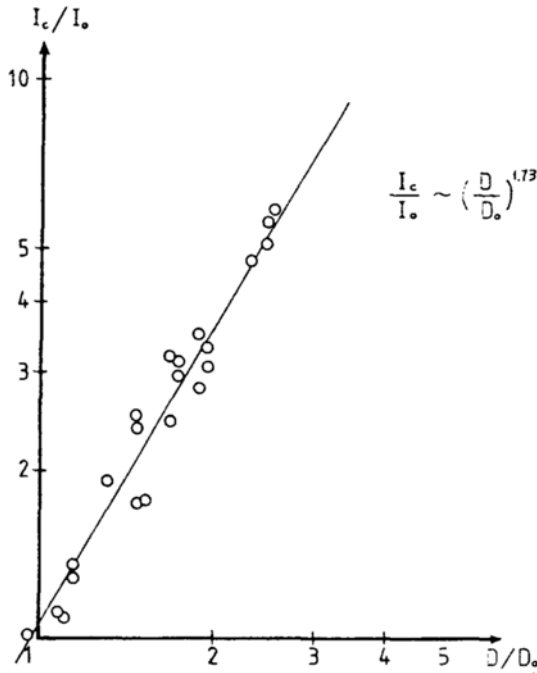


Fig. 4 Variation in the scattered light as a function of the particle diameter, for $\theta=10^\circ$

ellipsoids with their centers at 0 and their axes the same as the x, y, z , axes, the distribution of I/I_c can be approximated by

$$\frac{I}{I_c} = \text{Exp}\left\{-0.4\left(\frac{x^2}{\sigma_x^2} + \frac{y^2}{\sigma_y^2}\right)\right\} \quad (5)$$

In this particular case, $\sigma_x \approx 0.15\text{mm}$ and $\sigma_y \approx 3.5\text{mm}$ are representative orders of magnitude for these standard deviations, which shows that, in practice, the probe volume is and ellipsoid very much elongated along its y axis of revolution. The variation in I_c as a function of D was found by recording the light scattered by a series of balls of known diameters passing through the center of the equatorial plane. The results are given in Fig. 4.

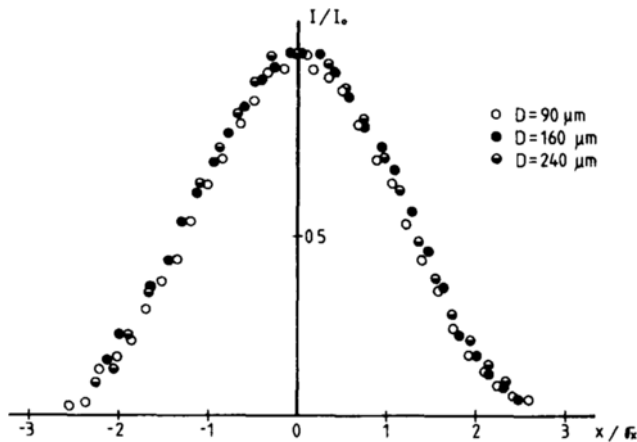


Fig. 5 Variation in the scattered light as a function of the point at which the particle passes through the equatorial plane, for $\theta=90^\circ$

The relation obtained is a power law with an exponent value compatible with the one that could be estimated from Mie's theory. Using Eq.(5), this gives us the experimental law:

$$\frac{I}{I_0} = \left(\frac{D}{D_0}\right)^{1.73} \text{Exp}\left\{-0.4\left(\frac{x^2}{\sigma_x^2} + \frac{y^2}{\sigma_y^2}\right)\right\} \quad (6)$$

If we set the angle of the PM axis in the same direction as the x axis (Fig. 1), the angle of observation θ is 90° . We can take advantage of the probe volume elongation along the y axis to eliminate the effect of this coordinate on the value of I . This can be done by limiting the field of the ellipsoid observed by the PM with a slit, on which the objective forms the image of the probe volume. The PM with a slit, on which the objective forms the image of the probe volume. The slit axis width is determined in such a way that it lets past only the light emitted from particles coming so close to the y - z plane that the light intensity is practically independent to y . The calibration measurements mentioned above are taken again for $\theta=90^\circ$ and are given in Figs. 5 and 6. We observe that the exponential part of I is the same as the one obtained for $\theta=10^\circ$, but the exponent of the power function of the diameter is 1.62, which is compatible with theory. (Brossmann, R., 1966)

The standard deviations of the scattered light distribution as a function of the x and y coordinates in the equatorial plane are not independent of the particle diameter because the dimensions of the particles used are not negligible in comparison with dimensions of the probe volume. Thus the relative variation in the incident light illuminating a particle increases with the size of the particle, which enlarges the probe volume as seen by the PM . The variation in σ_x as a function of D is measured for $\theta=90^\circ$, and is shown in Fig.

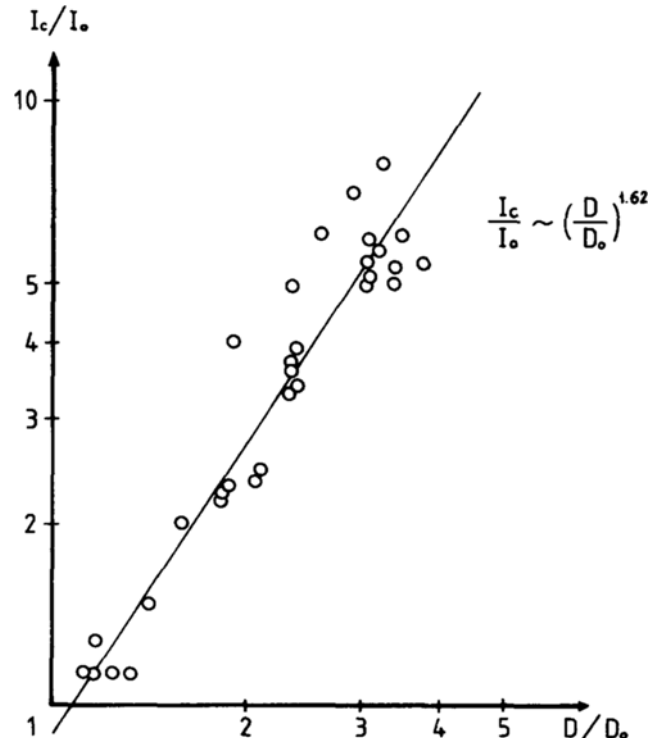


Fig. 6 Variation in the scattered light as a function to the particle diameter, for $\theta=90^\circ$

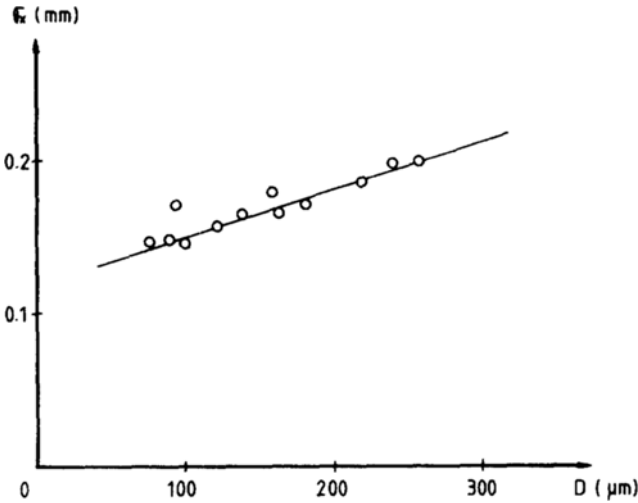


Fig. 7 Variation in the standard deviation σ_x as a function of the diameter for $\theta=90^\circ$

7. Figure 8 is the ratio of the peak intensity I to the intensity I_c of light scattered at the center when the PM is equipped with a slit. The probe volume is crossed at $x=0$.

The ideal distribution would be a vertical rectangle, but the diffraction in the slit and the finite size of the particle change the shape of the distribution. The phenomenon can be corrected in the measurements of I . Thus, when observing at an angle of 90° , a particle of diameter D passing through the equatorial plane of the probe volume at values of y between $-\ell$ and $+\ell$ scatters light at an intensity I given by:

$$\frac{I}{I_0} = \left(\frac{D}{D_0}\right)^{1.62} \text{Exp}\left(-0.4 \frac{x^2}{\sigma_x^2}\right) \quad (7)$$

If the particle goes beyond the interval $[-\ell, +\ell]$, the scattered light is occulted by the edges of the PM slit. Equation (7) determines the nature of the ambiguity in the interpretation of I , as there exists an infinite number of (x, D) couples giving the same peak value for I . When we want to find the probability density of D from that of I , this ambigu-

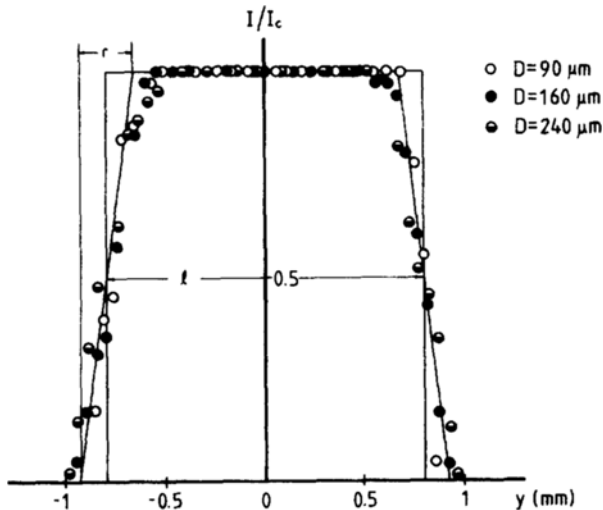


Fig. 8 Effect of the slit on the intensity of the scattered light

ity can be reduced relatively simply when certain conditions are fulfilled.

3. METHOD OF CALCULATING THE PROBABILITY DENSITY OF THE PARTICLE DIAMETERS

Here we take the case where the general relation $I=f(x, D)$ is not multiform in the considered domain. Let $p(I)$ be the probability density of I and let $p(x, D)$ be the related probability density of x and D . The probability that I will fall between two values, x and $x + \Delta x$, is given by the relation;

$$p(x < I < x + \Delta x) = \iint_{x < f(x, D) < x + \Delta x} p(x, D) dx dD \quad (8)$$

If the value I_1 , corresponds to x and I_2 corresponds to $x + \Delta x$, we have:

$$\int_{I_1}^{I_2} p(I) dI = \iint_{I_1 < f(x, D) < I_2} p(x, D) dx dD$$

If we allow that the particle diameter D is statistically independent of the position x where it crosses the equatorial plane, and furthermore that this position is a uniformly distributed variable (since no x can be preferred over another), we then have:

$$p(x, D) = p(x) p(D) = \frac{1}{\ell'} p(D)$$

where ℓ' is an equivalent length such that

$$\int_{-\infty}^{+\infty} \frac{dx}{\ell'} = 1 = \int_{-\infty}^{+\infty} p(x) dx$$

and $p(D)$ is the probability density of D .

It is also possible, for convenience, to represent $p(I)$ by a histogram of N classes with the class boundaries chosen in decreasing values I . The boundaries are denoted $I_0, I_1, I_2, \dots, I_j, \dots, I_n$, where I_0 is the highest observed light intensity and I_n is the instrument resolution threshold.

Let n_i be the value of $p(I)$ for the i -th class such that:

$$\int_{I_i}^{I_{i-1}} p(I) dI = n_i \Delta I_i$$

where $I_{i-1} - I_i = \Delta I_i$ and $\sum_{i=1}^N n_i \Delta I_i = 1$

The corresponding diameter distribution class boundaries can be calculated by drawing the curves $I=f(x, D)$ and selecting I as a parameter. The j -th boundary D_j will be given by $I_j = f(0, D_j)$. In effect, if I_0 is the highest peak value observed, this can only be due to the passage of the largest particle, of diameter D_0 , near the center, or roughly $x=0$. The first value I_1 may be due to particles of size D_1 passing through the center, or to larger particles passing farther away through the probe volume, and so forth. We can thus define a histogram of particle sizes broken down in two classes such that;

$$\int_{D_j}^{D_{j-1}} p(D) dD = n'_j \Delta D_j$$

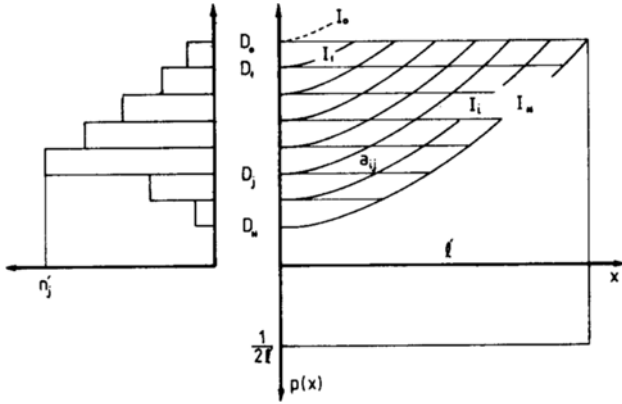


Fig. 9 Deconvolution principle

where $D_{j-1} - D_j = \Delta D_j$ and $\sum_{j=1}^N n_j' \Delta D_j = 1$

Figure 9 shows the variation of D as a function of x for several values of I . As the curves are symmetrical about D axis, only the curves for positive x values are shown. The D histogram and the uniform distribution of the x 's are shown opposite these curves. We can thus approximate the relation (8) with a discretized form giving, for example :

$$p(I_5 < I < I_4) = n_5 \Delta I_5 = \frac{1}{2\ell'} (a_{51}n_1' + a_{52}n_2' + a_{53}n_3' + a_{54}n_4' + a_{55}n_5')$$

or, more generally:

$$n_i \Delta I_i = \sum_{j=1}^i \frac{1}{2\ell'} a_{ij} n_j' \tag{9}$$

n_i and n_j are thus related by a system of linear equations of the form:

$$\begin{aligned} n_1 \Delta I_1 &= \frac{1}{2\ell'} a_{11} n_1' \\ n_2 \Delta I_2 &= \frac{1}{2\ell'} (a_{21} n_1' + a_{22} n_2') \\ n_3 \Delta I_3 &= \frac{1}{2\ell'} (a_{31} n_1' + a_{32} n_2' + a_{33} n_3') \\ &\vdots \\ n_N \Delta I_N &= \frac{1}{2\ell'} (a_{N1} n_1' + a_{N2} n_2' + a_{N3} n_3' + \dots + a_{NN} n_N') \end{aligned}$$

Equation (9) can be expressed in the matrix form:

$$[n \Delta I] = \frac{1}{2\ell'} [M][n']$$

Where $[n \Delta I]$ is a column matrix made up of elements calculated from experimental data, and $[M]$ is a triangular matrix made up of the elements a_{ij} calculated from the number of classes chosen and the system calibration relation.

we thus have: $[n'] = 2\ell' [M]^{-1} [n \Delta I]$

which thus makes it possible to calculate the particle size distribution from the I value distribution. This I distribution is found by processing the electrical signal from the PM , once

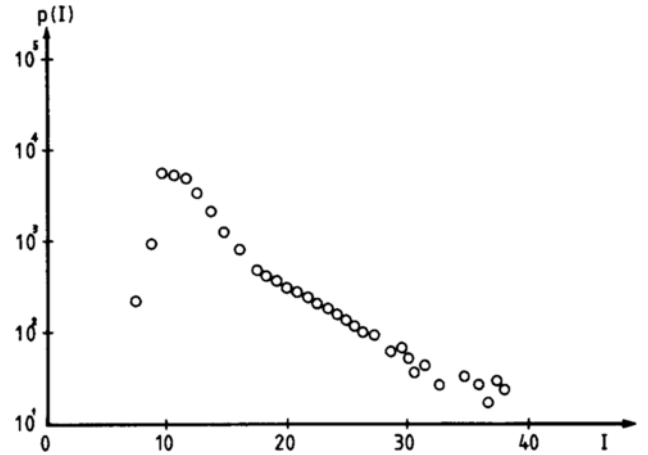


Fig. 10 Distribution of the scattered intensities (sample result)

the Doppler frequency signal is filtered out, with a multichannel DIDAC 800 analyzer to obtain directly a function proportional to the probability density of the peak values I . Figure 10 gives an example of the results obtained. The number of the channels in the abscissa is proportional to the probability density of the peak values I . Figure 10 gives an example of the results obtained. The number of the channels in the abscissa is proportional to the values of I . The proportionality constant is obtained from the system calibration. We then calculate the probability density of D by the method described above. Figure 11 shows the probability density calculated from the data in Fig. 10. The experiment is carried out using a set of glass balls with diameters ranging from 90 to 250 μm .

4. APPLICATION LIMITS AND ERRORS

A necessary condition for determining the particle diameter without ambiguity is that the $I = f(D)$ curve be monotonic. This curve is generally divided into three domains which, for the usual wavelengths of the lasers used, are the so-called "Rayleigh" domain for $D < 0.1 \mu\text{m}$, the "Mie" domain for $0.1 \mu\text{m} < D < 10 \mu\text{m}$,

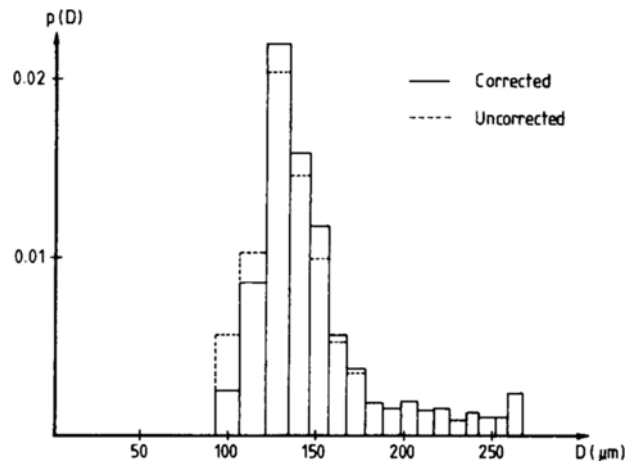


Fig. 11 Example of the diameter distribution data

and the geometric optical domain for larger diameters. Mie's more general theory covers the three domains and shows that I_c varies as D^6 in the Rayleigh domain but varies in the neighborhood of D^2 in the geometric optical domain. In the intermediate domain, the curve oscillates about a mean line of positive slope, and consequently makes the method unusable. In practice, the results is that the method is not applicable under the conditions existing with particles of less than $50 \mu\text{m}$. The upper limit is conditioned by the probe volume limitation. In the current measurement setup, a maximum size of $500 \mu\text{m}$ seems to be reasonable.

Consequently, the method proposed concerns particles going from 50 to $500 \mu\text{m}$. Within these limits, there exist two categories of errors inherent in the method: (1) Systematic errors, such as the edge effect error and coincidence error that can be corrected or controlled, and (2) random errors such as those introduced by the imprecision in the calibration. We can estimate these errors in the following ways.

The edge effect error (see Fig. 8) is due to the fact that the distribution of the scattered light is not a perfect rectangle. Because of the finiteness of the particles and also probably because of the diffraction from the PM slit, the light decreases from the constant value it maintains in the center of the probe volume, tending to cancel out toward the outside. Thus there exist two lateral areas of roughly equal widths in which I/I_c is a function of x and y simultaneously. This phenomenon can be taken into account by first calculating the matrix $[M]$, which assumes that the distribution is a perfect rectangle of mean width ℓ and then adding a correction matrix estimated on basis of a linear decrease in the light intensity as a function of y over a width v , for which we have verified that the value is practically independent of ℓ . The result of the correction can be seen in Fig. 11.

Another source of error, the coincidence error, is caused by the simultaneous presence of several particles in the probe volume. When this happens, the observed pedestal signal is the result of several superimposed elementary signals and becomes much more complicated to interpret. This source of error depends on the mean particle concentration c and the dimensions of the probe volume. In effect, the probability $p(K)$ that K particles will appear simultaneously inside the probe volume V_0 is given by a Poisson distribution:

$$P_{V_0}(K) = \frac{(cV_0)^K}{K!} e^{-cV_0}$$

To avoid the coincidence error, it is preferable that the probability of finding two particles simultaneously in V_0 be much lower than the probability of finding just one. The calculation yields:

$$\frac{P_{V_0}(2)}{P_{V_0}(1)} \ll 1 \rightarrow cV_0 \ll 2$$

For these experiments, we can estimate V_0 at $0.5 \times 10^{-3} \text{cm}^3$ and c at some 50 particles per cubic centimeters. We get the value 0.023 or V_0 , which is acceptable. When the concentration is too high, we can reduce V_0 , but this increases the edge effect. Furthermore, and imprecise experimental determination of the exponent α in the Eq. (4) can also introduce an error, though this is generally rather small. In effect, for particles passing through the center of the probe volume, we have:

$$D = D_0 \left(\frac{I}{I_0} \right)^{\frac{1}{\alpha}}$$

which gives :

$$\left| \frac{\Delta D}{D} \right| = \left| \frac{1}{\alpha} \ell n \left(\frac{I}{I_0} \right) \frac{\Delta \alpha}{\alpha} \right|$$

If we choose I_0 and D_0 at the center of the observe interval of values, the maximum deviations occur at the extremities of the interval. Typically, it can be seen that for an error $\Delta \alpha / \alpha$ of 10%, the relative error $\Delta D / D$ in the measurement of D is also on the order of 10%.

The method for determining the particle size assumes that the particles are spherical. Consequently, the balls selected for the various calibrations are selected according to this criterion. Yet the light scattered from a series of randomly chosen balls of various diameters, placed at the center of the probe volume, is measured while rotating them about their center. We thus found an invariance in rotation for the largest particles, but deviations reaching 50% for the smallest ones. This last effect is perhaps amplified by a variation in the position of the ball center during the rotation, which has a greater effect on the smaller particles. This results in an imprecision that is difficult to estimate in the $p(I)$ distribution and thus in $p(D)$.

5. CONCLUSION

The proposed method of measuring the size distribution of spherical particles has the advantage of using a conventional Doppler effect laser anemometer setup. It requires only a filtering of the signal from the PM terminals to remove the Doppler signal, which can be processed elsewhere simultaneously, and retain only the pedestal. The principle consists of observing the probe volume along the smallest axis parallel to the interference fringes in this volume and taking advantage of its relative elongation to eliminate one of the space coordinates. Furthermore, the only quantity of interest is the peak value of the pedestal signal, the intensity of the light scattered by the particle when it passes through the equatorial plane. This intensity thus depends only on two variables: the abscissa of the point where the particle crosses this plane and the diameter of the particle. The relationship between this peak value and variables previously mentions can be done *in situ*. This calibration is used to calculate the size probability density from the peak value probability density, which can be found rather simply when the frequency band of the pedestal permits, as is the case here.

The method for calculating the size distribution is based on a discretization of the problem that is convenient in programming the calculations, and on the uniform distribution of the particle passage through the equatorial plane. The results obtained by this method compare satisfactorily with a directly measured size distribution. The method is only applicable in the so-called geometric optical domain of, considering the wavelength of the laser used, for particles from 50 to $500 \mu\text{m}$. The upper limit depends on the dimensions of the probe volume.

To avoid having two or more particles in the probe volume at the same time, which makes the signal difficult to interpret, it is better that the concentration not be too high. Similarly, the probe volume should be the minimum compat-

ible with the size of the largest particles appearing in the experiment. The calibration errors are not extremely important. On the other hand, the effect of the non-sphericity of the particles may introduce an error that is difficult to evaluate but it does not seem to be negligible for small particles, where it may distort the distribution.

Finally, the relative simplicity of implementing this method makes it useful whenever a direct calibration is possible.

REFERENCES

- Brossmann, R., 1966, "Die Lichtstreuung an kleine Teilchen als Grundlage einer Teilchengrößenbestimmung", Diss, Th., Karlsruhe.
- Farmer, W.M., 1972, "Measurement of Particle Size, Number Density and Velocity Using a Laser Interferometer", *Appl. Optics*, Vol. 11, No. 11, p. 260.
- Mie, G., 1908, "Beiträge zur Optik Trüber Medien, Speziell Kolloidaler Metallösungen", *Ann. Physik*, 4, Bd 25.
- Umfauer, H., 1975, "Ermittlung von Partikel-größenverteilungen in Aerosolströmungen hoher Konzentration mit Hilfe einer Sterulichtmesseinrichtung", VDI, Bericht, No. 232.
- Van de Hulst, H. C., 1957, "Light Scattering by Small Particles", John Wiley and Son, New-York.
- Yoon, S. J., 1984, "Méthode Optique de Mesure de la Granulométrie et du Coefficient de Corrélation Locaux d'un Aérosol", Rapport de D.E.A., I.M.F.S., Strasbourg.
- Yule, A.J., et al., 1977, "Particle Size and Velocity Measurement by Laser Anemometry", *J. of Energy*, Vol. 1, No. 4, pp.220~228.